Nucleic Acids Research, 1996, Vol. 24, No. 7 **1187–1194**

The use of non-uniform deuterium labelling ['NMR-window'] to study the NMR structure of a 21mer RNA hairpin

A. Földesi, S.-I. Yamakage, F. P. R. Nilsson, T. V. Maltseva and J. Chattopadhyaya*

Department of Bioorganic Chemistry, Box 581, Biomedical Center, Uppsala University, S-751 23 Uppsala, Sweden

Received January 26, 1996; Revised and Accepted February 19, 1996

ABSTRACT

The first synthesis of a non-uniformly deuterium labelled 21mer RNA is reported using our 'NMR-window' concept, showing its unique application in the unambiguous NMR assignment of the non-exchangeable aromatic and sugar protons.

INTRODUCTION

As the number of nucleotide residues increases in an oligo-DNA or RNA, the use of high-field NMR spectroscopy in the elucidation of the structure and dynamics poses severe problems because of the spectral overlap caused by the repeating nucleotide units, the line-broadening due to decreased T_2 relaxations (1), and a slower tumbling rate finally causes an increase in T_1 relaxation (1). It has only recently emerged that one way to overcome this inherent size limitation problem is the development of isotope labelling techniques. Enormous efforts have thus been invested in the enzyme promoted synthesis of uniformly $^{13}C/^{15}N$ labelled RNA and their structure elucidation using triple resonance spectroscopy (2–4). We, on the other hand, have developed synthetic methodologies for specific deuteration of nucleosides, which are then incorporated into the specific domains of an oligonucleotide using solid phase synthesis protocol in a non-uniform manner to solve the overcrowding problem in their ^{1}H-NMR spectra (5–9). Thus these synthetic partially-deuterated oligonucleotides have a ^{1}H-NMR-invisible part and a short ^{1}H-NMR-visible part ('NMR window'), which is then used to extract structural information (Fig. 1; 5,6). We have earlier demonstrated (7,8) the application of this unique 'NMR window' concept on a self-complementary 20mer DNA, showing that the overcrowding of proton resonances in the NMR-window part is considerably reduced, thereby enabling us to assign proton resonances to determine the NOE volumes as well as the $^3J_{HH}$ couplings accurately (9).

We herein show for the first time that this '^{1}H-NMR window' concept is equally applicable in the NMR studies of large oligo-RNA as exemplified by a comparative study with a natural 21mer (Fig. 1a) and its deuterated analogue (Fig. 1b). It has been demonstrated in this work that it would have been very difficult to assign the resonances of the natural 21mer RNA (Fig. 1a) without the direct help of the deuterated 21mer analogue (Fig. 1b).

MATERIALS AND METHODS

The deuterium labelled 2′,3′,4′$^{\#}$,5′,5″-$^2H_5$-β-D-ribonucleoside derivatives (Fig. 1c) were prepared by our published procedure [5,6; further improved unpublished preparation protocol for the deuterated sugar and the deuterated nucleoside blocks are available from the authors' lab (Fax: +46 1855 4495; e-mail: Jyoti@BioorgChem.uu.se)]. Triethylamine trihydrofluoride (10) was purchased from Aldrich. 1,3-Dichloro-1,1,3,3-tetraisopropyldisiloxane (11) and 2-cyanoethyl *N*,*N*-diethyl-chlorophosphoramidite (12) were prepared using literature procedures. Analytical TLC was carried out using Merck pre-coated Kieselgel 60 F_{254} glass backed plates. Kieselgel G60 from Merck was used for short column chromatographic separations. DEAE-Sephadex G-25 super fine, DNA grade (Pharmacia, Sweden) was used for gel filtrations.

Deuteration of C-5 position of uridine (13) and its conversion to C-5 deuterated cytidine (14), protection of different nucleobases (benzoyl for A and C and phenoxyacetyl for G) (15,16) and *tert*-butyldimethylsyilyl for 2′-OH hydroxyl functions (17), phosphitylation of 3′-OH (18,19) of 5′-DMTr base protected deuterium labelled ribonucleoside blocks by 2-cyanoethyl *N*,*N*-diethyl-chlorophosphoramidite were achieved by published procedures (20,21). All building blocks were satisfactorily characterized by ^{1}H- and ^{31}P-NMR. The ^{31}P chemical shifts for the natural and deuterated phosphoramidites were within the experimental error.

RNA synthesis and purification

The natural and deuterium labelled 21mer RNAs were prepared by the solid phase phosphoramidite method on an ABI DNA/RNA synthesizer model 394 equipped with eight ports for the addition of the four natural and four sugar deuterated phosphoramidite blocks for the synthesis of the deuterated 21mer (Fig. 1b). The standard programs for 1.0 µmol scale RNA synthesis from ABI were used in a way to have 10 min coupling time (1 µmol

* To whom correspondence should be addressed

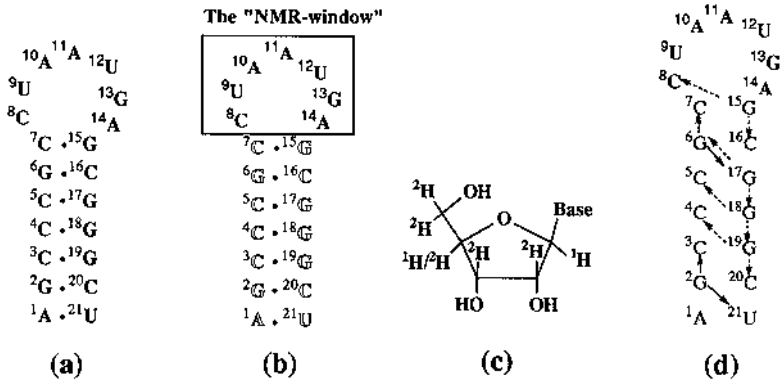

Figure 1. (**a**) The natural 21mer hairpin RNA. (**b**) The partially-deuterated analogue of 21mer RNA incorporating deuterated blocks as shown in (**c**), where Base = adenin-9-yl, guanin-9-yl, C5-^{2}H-cytosin-1-yl or C5-2H-uracil-1-yl (>95% ^{2}H enhancements). The partially-deuterated blocks are located in the stem region and are shown in the 'outline' font and the nucleotides in the 'NMR-window' region is shown in 'bold' font in (b). The partially-deuterated sugar residues shown in (c) for specific incorporation into the 21mer RNA using our 'NMR-window' approach (5–9) has the following deuterium enrichments: >97 atom %^{2}H at H2′, H3′ and H5′/5″ sites, ~65 atom % ^{2}H at H4′. (**d**) The arrows show the observed NOE connectivities between base-paired G imino protons and sugar H1′ of the 3′-end of the same strand as well as to H1′ of the 3′-end of the opposite strand denoting the A-type RNA in the stem region of 21mer (32).

scale × 12 syntheses). After deprotection in saturated ethanolic ammonia for 7 days at ambient temperature, the solvent was evaporated. The residue was redissolved in neat triethylamine trihydrofluoride and stirred for 17 h at ambient temperature. After 17 h, the mixture was desalted by using a Sephadex G 25 gel filtration column. The crude mixture was analysed by reversed phase HPLC and the peak for the main product (R_t = 46 min) was integrated for 78.5% giving an average coupling yield of ~99%. Purification of the oligomers was carried out by preparative reversed phase HPLC (Gilson system consisting of Model 305 & 306 Pumps, 811C Dynamic Mixer and 118 UV Detector) on a Kromasil 100-5C18 (250 × 8 mm^2) reversed phase column with a linear gradient of 0→30% buffer B (0.1 M TEAA pH 6.8, 50% CH_3CN) in buffer A (0.1 M TEAA pH 6.8, 5% CH_3CN) over a period of 50 min with a loading of 25 OD units of crude RNA per injection. Appropriate peaks were collected and evaporated. The purified residue was co-evaporated with double distilled H_2O several times and loaded to Dowex 50 WX (Na^+ form).

Preparation of NMR sample

Finally, samples (~200 OD units each) were lyophilized to dryness several times from D_2O. The solid powder of the natural or deuterated 21mer RNA was then dissolved in 0.5 ml of H_2O or D_2O buffer containing 100 mM NaCl, 10 mM NaD_2PO_4, 10 µM EDTA and 0.02% NaN_3 (pH 6.5) for NMR measurements. The final concentrations of the samples were ~1.6 mM.

Nuclear magnetic resonance spectroscopy

^{1}H-NMR spectra were recorded on a Bruker AMX 500 NMR spectrometer (^{1}H at 500.13 MHz). Phase-sensitive NOESY experiments (22) were performed at 21°C using the following parameters: mixing time 0.3 and 0.6 s, 4K complex data points in t_2, 512 complex data points in t_1, a relaxation delay of 5.0 and 3.5 s, a sweep width of 5050.5 Hz in both dimensions, acquisitions per FID was 128; a shifted squared sine-bell apodization function was applied for both dimensions. The data were zero-filled in t_1 to give 2K × 1K complex data points. The residual water resonance was saturated during the relaxation delay. Two-dimensional data sets for DQF-COSY (23) spectra were collected in the phase-sensitive mode with the time-proportional phase incrementation with phosphorus decoupling. Typically 4096 data points were collected for each 512 t_1 values in DQF-COSY experiments. The 4096 × 512 data points were resolution enhanced by a shifted squared sine-bell window function in both t_1 and t_2 directions, then Fourier transformed and phase adjusted, a relaxation delay of 3 s was used. The data were collected with the non-spinning sample to avoid t_1 noise. The NOESY experiments in 90% H_2O/10% D_2O mixture (24) at 5 and 21°C (with mixing time of 0.3 and 0.6 s, relaxation delay of 2.5 s) were performed with a final spectra of 2K × 1K real data points after Fourier transformation. The spectra in 90% H_2O/10% D_2O mixture were corrected for the excitation profile (24). One-dimensional experiments in aqueous solutions were performed by using the pulse sequence 45–t_m–45 (t_m = 195 µs, relaxation delay of 10 s) with a sweep width of 5050.5 Hz.

RESULTS AND DISCUSSION

The sequence and a possible folded 2D structure of 21mer RNA (Fig. 1a) corresponding to residues 114–134 within the *trp* leader mRNA transcript in *Escherichia coli* has been thought to provide the termination and the anti-termination signals recognized by RNA polymerase. Hence, attempts have been made earlier to study this G-C rich 21mer by 600 MHz NMR (25), where the imino protons were clearly observed but could not be assigned because of the spectral overcrowding in the aromatic, anomeric and other regions where other aliphatic sugar protons absorb. These considerations led us to decide to use this 21mer hairpin RNA to show the applicability of our 'NMR-window' concept.

The imino proton resonances in 1D spectra at 500 MHz is shown in Figure 2a, which is the same both for natural and the deuterated 21mer RNA. The appearance of relatively sharp imino proton resonances for the 21mer RNA in the downfield region shows that they arise due to the hydrogen-bonded helix as shown in Figure 1a or b. The assignment of the imino proton resonances shown in Figure 2a and c is based on the comparative analysis of the NOESY spectra of both for the natural and the deuterated sample at 5 and 21°C in H_2O and D_2O (*vide infra*). Unlike earlier

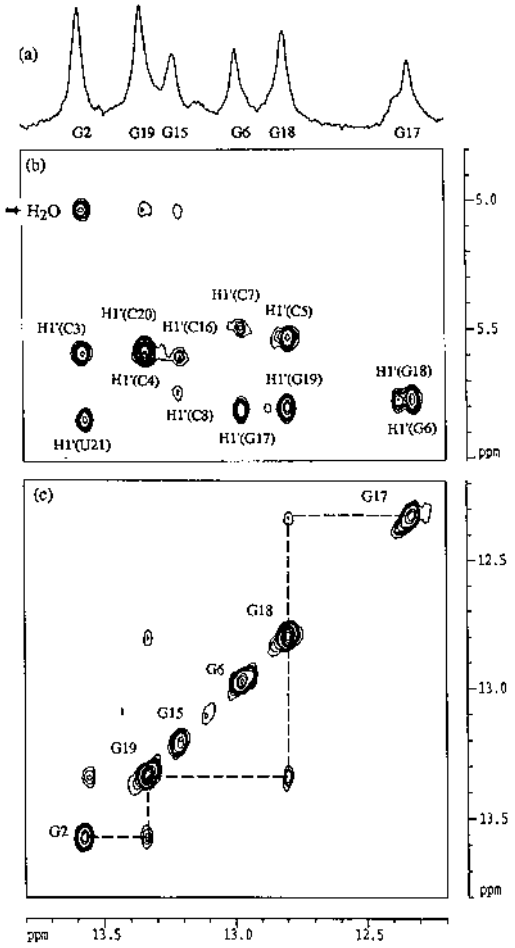

Figure 2. (**a**) Resonances of imino protons from the 1D ^{1}H-NMR of the deuterated analogue of the 21mer RNA (Fig. 1b) in H_2O-D_2O (90:10%, v/v) containing 100 mM NaCl, 10 mM NaD_2PO_4, 10 μM EDTA and 0.02% NaN_3 (pH 6.5) at 5°C. (**b**) The imino-anomeric and (**c**) the imino-imino regions of the NOESY spectrum of the deuterated 21mer RNA at 5°C. The imino-imino walk from G2 to G17 is traced with a dashed line. The diagonal peaks in 2D NOESY in (c) and imino proton resonances in 1D spectrum in (a) are marked by numbered capital letters as shown in Figure 1a. The cross-peaks between imino protons and H1′ of the next residue both at the 3′-end of the same strand and at the 3′-end of the opposite strand are observed and marked, thereby establishing the connectivities in Figure 1d.

work (25), we have observed sequential imino–imino cross connectivities (Fig. 2c) at both 5 and 21°C in the NOESY spectra at 300 and 600 ms mixing time, but they could not be assigned easily without the knowledge of the assignment of aromatic-H1′ region (*vide infra*). Here, we faced one of the most complex problems involving the elucidation of the starting point of the NMR assignment task, which is often one of the most difficult issues to solve in RNA structure determination (26). We assumed that since the most downfield imino proton resonance at 13.56 p.p.m. at 5°C rapidly exchanges with the bulk water, and this is also the first signal that disappears from the NOESY spectrum as the temperature of the sample is increased, this peak could be either from the 3′-terminal G2 residue or from G15 (the closing base-pair which is a part of the loop). On the other hand, the most upfield imino proton resonance at 12.32 p.p.m. is a nice candidate for the terminal imino proton of the G2 or G15 residue to start the sequential walk since this peak is rather broad compared with any other imino resonances but the problem is that this imino resonance exchanged very slowly compared with the resonance at 13.56 p.p.m. This problem could not be simply resolved by looking at the imino–imino and imino–H1′/H5 region of the NOESY spectra. It only could be unambiguously tackled by looking at the aromatic-H1′ as well as other NOE cross-connectivities of the non-exchangeable protons in the deuterated 21mer.

Figures 3, 4 and 5 show expanded parts of 2D NOESY spectrum of the natural and the deuterated analogue of 21mer RNA. Their aromatic-H1′ region is found to be reasonably well dispersed (compare Fig. 3a and b). On the other hand, the H2′, H3′, H4′ and H5′/5″ regions of the natural 21mer are far more crowded compared with the corresponding regions in the deuterated counterpart (compare Fig. 4a with b and Fig. 5a with b). In order to design an appropriate deuterated analogue of the 21mer RNA in such a manner that the starting point of our NMR assignment of the non-exchangeable protons could be fixed in advance, we chose the following strategy. Since all adenine aromatic protons are normally more downfield than other aromatics, we found that all H8-H1′ cross-peaks of all four A residues (A1, A10, A11 and A14) of 21mer were dispersed and observed in the downfield region of the spectra (Fig. 3a). Hence, we chose to incorporate the deuterated nucleotide residues (Fig. 1c) in the whole stem region that covers only one adenine nucleotide (i.e. A1) at the 3′-terminus as shown in Figure 1b. Since these deuterated blocks (Fig. 1c) have H1′ residual proton but not H2′ (see Fig. 1 legend for details), hence by examination of the DQF-COSY spectra (compare Fig. 6a with b) of the natural versus the deuterated 21mer RNA, we found that the cross-peak H1′-H2′ of A1 residue has vanished whereas the H1′-H2′ cross-peaks for A10, A11 and A14 in the loop part are clearly observed. This strategy also worked very well for the U21 residue, which could be assigned unambiguously from the comparison of the DQF-COSY spectra of natural and deuterated RNA, and hence it could also be used as the starting point for the assignment. This approach could be of considerable importance as a general strategy for establishing the starting point for the assignment of resonances of large RNA since the terminal nucleotide residue will be expected to always have a preference for the S-type conformation. Hence if we incorporate a deuterated block such as shown in Figure 1c at this position, we would always observe the disappearance of the H1′-H2′ cross-peak in the DQF-COSY spectra compared with the natural counterpart.

One other important point about incorporating the deuterated block such as shown in Figure 1c in the synthesis of the non-uniformly deuterated 21mer analogue (Fig. 1b) is as follows. In the natural 21mer, the NOE cross-peaks for $(H1'\text{-}H8/H6)_i$ and $H1'_{i-1}\text{-}H8/H6_i$ in the aromatic-H1′ region were obscured by H5-H6 cross-peaks, which added more complexity to our problem for further assignment. This is evident from a comparison of a sequential walk from G2 to G6 and C8 to U9 residues in Figure 3a and b, which was solved by 95% ^{2}H enrichment at the C5 of uracil (27–31) and cytosine (31) residues as shown in Figure 1c and incorporating them in the stem part of the deuterated RNA (Fig. 1b). Thus the H5-H6 cross-peaks for those deuterated residues vanished in the NOESY and DQF-COSY spectra (compare Fig. 3a with b and Fig. 7a with b).

Figure 3a and b shows the aromatic-H1′/H5 region of the NOESY spectrum of the natural 21mer and its deuterated analogue. It can be seen from a comparison of Figure 3a with b

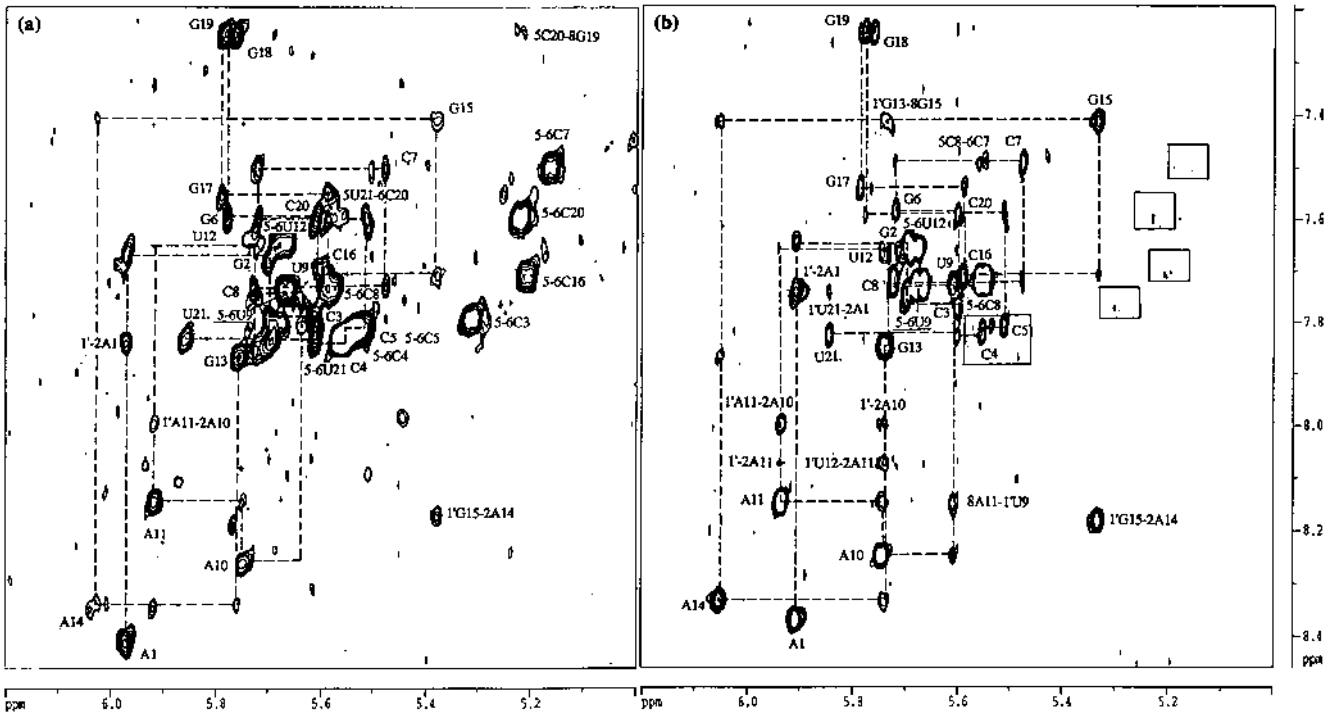

Figure 3. For the sake of comparison, identical regions of the NOESY spectra correlating between aromatic and anomeric H1′ resonances are shown in (**a**) for natural 21mer RNA (Fig. 1a) and in (**b**) for the partially deuterated 21mer RNA analogue (Fig. 1b), which have been acquired in ^2H_2O at 24°C. The dashed lines connect the NOE cross-peaks between H1′ and H8/H6, which are observed in both (a) and (b) starting from the A1 residue. The cross-peaks belonging to $(H1'\text{-}H8/H6)_i$ intraresidual protons are marked by numbered capital letters as shown in Figure 1a. The cross-peaks showing interaction between aromatic H5 and H6 proton of cytosine or uracil are marked when they are visible. Since H5 proton in uracil and cytosine has been substituted by deuterium in the deuterated analogue (Fig. 1b), the H5-H6 cross-peaks for these deuterated pyrimidine residues are only very faintly observed (>95%^2H enhancement at C5), which are shown by empty square boxes. Note that the assignment of the aromatic-H1′ cross-peaks for C3, C4, C5 and U9 residues in natural 21mer RNA in (a) has been achieved with the help of the deuterated analogue as shown in (b). The small differences in the chemical shifts between the natural 21mer, spectrum (a), and its partially-deuterated analogue, spectrum (b), result from small differences in the concentration.

that the sequential connectivities in the deuterated 21mer in Figure 3b are easily traced starting from the intraresidual $(H1'\text{-}H8)_i$ cross-peak of A1 to all other residues without any problem because of absence of H5-H6 cross-peaks of C4, C5 and U21, and are summarized in Table 1. The NOESY spectrum at 300 ms mixing time had numerous aromatic/aromatic cross-peaks (data not shown) that also support the assignments shown in Table 1.

The aromatic H6/H8 to H2′, H3′, H4′, H5′ and H5″ region in the natural 21mer of RNA (Fig. 4a) was found to be overcrowded from the overlapping sugar resonances due to the isochronous chemical shifts of the H2′, H3′, H4′, H5′ and H5″ protons for most of the nucleotide residues (see the box in Fig. 4a). This makes the sequential walk from $(H2'\text{-}H8/H6)_i$ to $H2'_{i-1}\text{-}H8/H6_i$ and from $(H3'\text{-}H8/H6)_i$ to $H3'_{i-1}\text{-}H8/H6_i$ almost impossible even for those nucleotides in the loop part where the chemical shifts of aromatic protons of A10, A11 and A14 are shifted downfield (Fig. 4a). The situation is, however, dramatically changed in case of the deuterated analogue of 21mer RNA (compare Fig. 4a with b) in which many cross-peaks for H6/H8 to H2′, H3′, H4′, H5′ and H5″ have become well resolved (see the box in Fig. 4b), and therefore they could be sequentially traced from C8 to G15 residues in the non-deuterated loop very easily. It is noteworthy that the H3′ resonances are shifted more downfield than H2′ resonances for A11, G13, C8, U9 and U12 residues, whereas this is reversed for A10 and A14 residues. From the aromatic-aromatic cross-peaks, we see, however, that all loop residues are well stacked (data not shown). Hence, without a full structural refinement, we are unable to point out why the chemical shifts of H2′ and H3′ in the loop residues are reversed.

The expanded H1′/H5 to its own H2′, H3′, H4′, H5′ and H5″ NOESY regions for the natural and the deuterated 21mer RNA are shown in Figure 5a and b, respectively, and when resolved they are connected by straight horizontal lines. The crowded area in the NOESY spectra for the natural 21mer is shown in the boxed area in Figure 5a, which can be seen to be much simplified in the deuterated 21mer as shown in Figure 5b. A perusal of Figure 5b for the deuterated 21mer shows that each H1′ of seven non-deuterated nucleotide residues in the loop has exhibited cross-peaks with its own H2′, H3′ and H4′. The assignment of the H2′ resonances of loop is achieved from the H1′-H2′ cross-peaks observed in DQF-COSY spectrum (Fig. 6b), which is confirmed by the sequential walk from $(H2'\text{-}H8/H6)_i$ to $H2'_{i-1}\text{-}H8/H6_i$ (Fig. 4b). Assignment of the H3′ and H4′ resonances was achieved primarily from the cross-peaks between H3′-H4′ in DQF-COSY spectrum (data not shown), and also confirmed by the sequential walk from $(H3'\text{-}H8/H6)_i$ to $H3'_{i-1}\text{-}H8/H6_i$ (Fig. 4b). The H2′, H3′, H4′, H5′ and H5″ of the stem part of the natural 21mer RNA could not be assigned due to severe overlap of their H1′ chemical shifts (see the box in Fig. 5a). This problem could not be tackled with the present deuterated 21mer since all stem residues were deuterated, and hence they were not ^1H-NMR observable. The

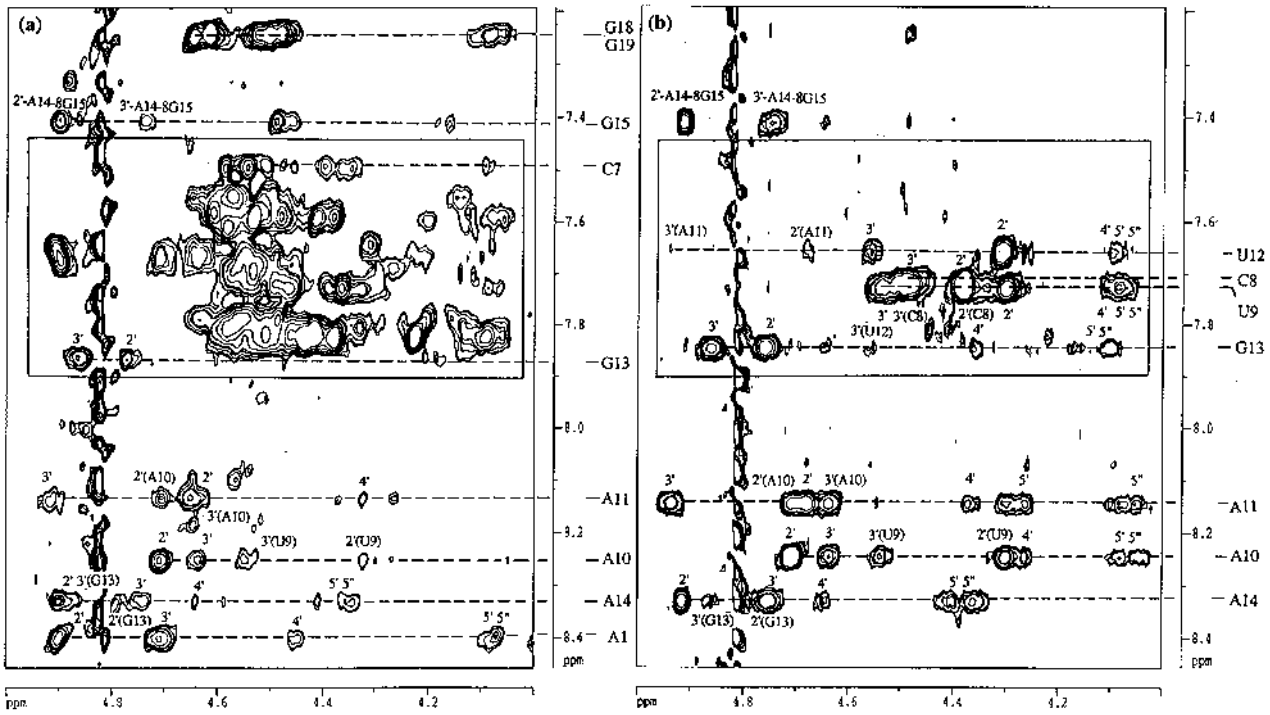

Figure 4. A comparative analysis of the NOESY spectra of aromatic to H2′/H3′/H4′/H5′/H5″ region for the natural 21mer RNA (Fig. 1a) in (**a**) and its deuterated analogue in (**b**) in ^2H_2O at 24°C is shown. A comparison of the boxed areas in (a) and (b) shows that a significant number of resonances that were overlapping or nearly overlapping in this region for natural 21mer RNA in (a) are now well resolved in case of the corresponding deuterated analogue in (b). The cross-peaks belonging to the same residue are connected by dashed lines and the appropriate assignments have been labelled.

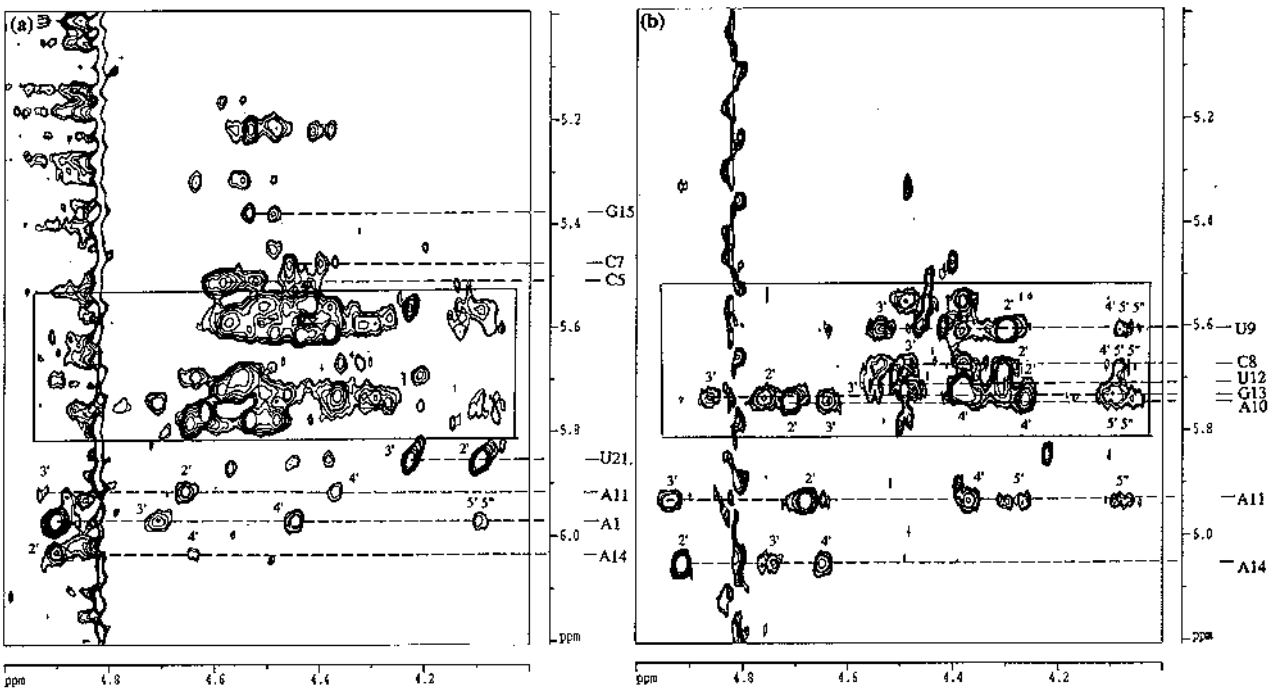

Figure 5. A comparative analysis of the NOESY spectra of H1′/H5 with the H2′/H3′/H4′/H5′/H5″ region for the natural 21mer RNA (Fig. 1a) in (**a**) and its deuterated analogue in (**b**) in ^2H_2O at 24°C is shown. A comparison of the boxed areas in (a) and (b) shows that a significant number of resonances that were overlapping or nearly overlapping in this region for natural 21mer RNA in (a) are now well resolved in case of the corresponding deuterated analogue in (b). The cross-peaks belonging to the same residue are connected by dashed lines and the appropriate assignments have been labelled.

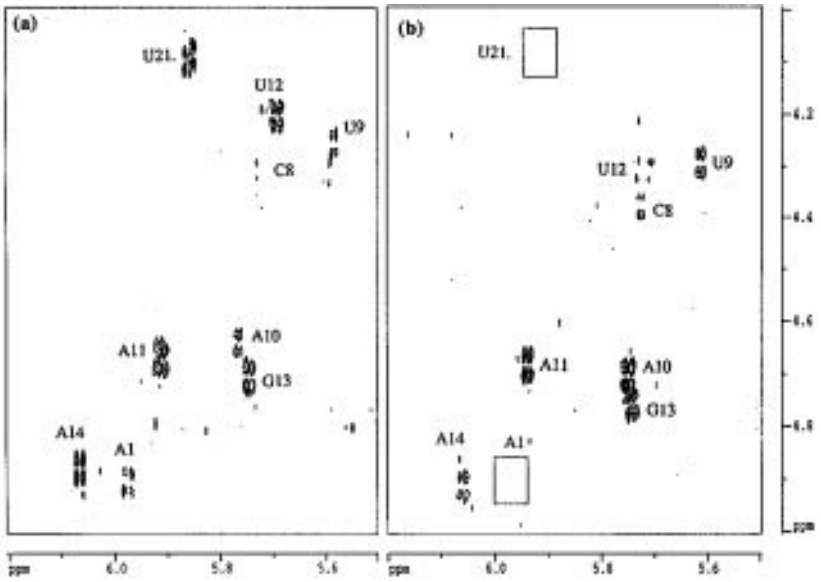

Figure 6. A comparison of contour plots of the DQF-COSY spectra in ^2H_2O at 24°C, showing the H1′-H2′ region for the natural 21mer RNA in (**a**) and its deuterated analogue in (**b**). This shows that the H1′-H2′ cross-peak for the terminal A1 and U21 residues found in the natural 21mer in (a) has vanished in the spectrum of the deuterated analogue in (b) because these residues are deuterated. Note that the sugars in the loop preferably adopt S-type conformation, and hence their H1′-H2′ cross-peaks are easily observed in the spectra of both natural and deuterated 21mer RNA. It may also be noted that the last ^7C-^{15}G base-pair of the stem, which is also a part of the loop, is however in the N-type conformation as the rest of the residues of the stem as evident by the absence of their H1′-H2′ cross-peaks. The small differences in the chemical shifts between the natural 21mer, spectrum (a), and its partially-deuterated analogue, spectrum (b), result from small differences in the concentration.

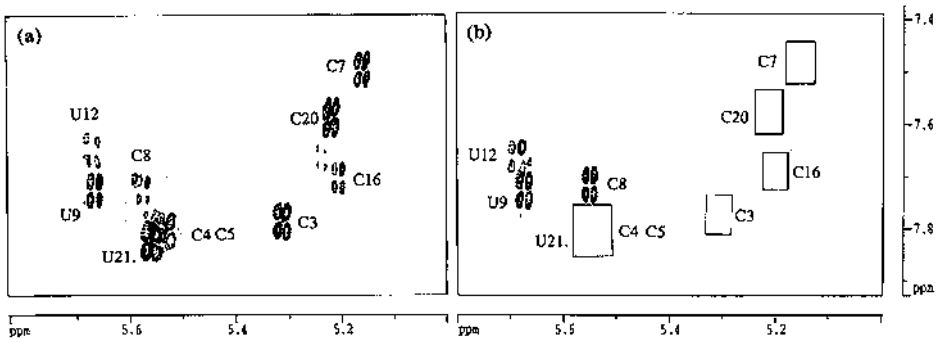

Figure 7. Comparison of contour plots of the DQF-COSY spectra in ^2H_2O at 24°C, showing the H8/H6-H1′/H5 region for the natural 21mer RNA in (**a**) and its deuterated analogue in (**b**). It can be seen that only three H5-H6 cross-peaks belonging to three pyrimidine residues of the loop (U12, U9 and C8) are visible in the spectrum of the deuterated analogue (b), whereas all H5-H6 cross-peaks of all pyrimidine residues (i.e. C3, C4, C5, C7, C16, C20 and U21) are observed in the natural 21mer RNA as seen in (a).

obvious solution to this problem is to synthesize a second deuterated analogue of the 21mer RNA in which the loop part should be deuterated and the stem part should be left natural.

Having achieved the assignment of all H1′ resonances of all nucleotide residues of the 21mer RNA, our next step was the identification of NOE connectivities between base-paired G imino protons and the sugar H1′. We expected (32) that the NOE cross-peaks for a typical A-type RNA should arise through a pathway from G(imino)–G(hydrogen-bonded amino)–G(non-hydrogen-bonded amino) to both the H1′ of 3′-end of the same strand and of the opposite strand (see Fig. 1d). Indeed, Figure 2b shows two NOE cross-peaks for every imino proton in the H1′/H5 region for the deuterated 21mer because the resonances from H5 to imino proton through the pathway G(imino)–C(hydrogen-bonded amino)–C(non-hydrogen-bonded amino) to H5 are not observed in this imino-H1′/H5 region of spectrum because of C5 deuteration. In the same part of spectrum, however, all three cross-peaks have been detected from the fully protonated 21mer RNA (data not shown). Since the imino proton of G2 is expected (Fig. 1d) to show two cross-peaks from imino(G2) to H1′(U21) and from imino(G2) to H1′(C3), and this has indeed been found (Fig. 2b), the resonance at 13.47 p.p.m. has been unambiguously assigned to the imino proton of the G2 residue. This assignment has been further confirmed by the sequential walk through imino-imino protons (see Fig. 2c).

Table 1. Chemical shifts of the aromatic (H8/H6/H5/H2), sugar H1′, H2′, H3′ and H4′, 5′/5″ protons and exchangeable imino and amino protons at 21°C based on NOESY and DQF-COSY data of both natural and the deuterated 21mer RNA

Residue	H8/H6	H5/H2	H1′	H2′	H3′	H4′	H5′,H5″	NH	NH_2
^{1}A	8.36[a]	7.36[a]	5.91[a]	4.90[a]	4.70[a]	4.38[a]	4.08, 3.98[a]	f	h
^{2}G	7.64[a]	f	5.70[a]	b	b	b	b	13.47[e]	h
^{3}C	7.76[a]	5.29[c]	5.60[a]	b	b	4.39[a]	b	f	8.68[e], 6.87[e]
^{4}C	7.82[a]	5.54[c]	5.55[a]	b	b	4.38[a]	b	f	8.52[e], 6.88[e]
^{5}C	7.80[a]	5.52[c]	5.51[a]	b	b	4.44[a]	b	f	8.37[e], 6.74[e]
^{6}G	7.58[a]	f	5.72[a]	b	b	4.48[a]	b	12.91[e]	h
^{7}C	7.49[a]	5.16[c]	5.47[a]	b	b	4.39[a]	b	f	8.39[e], 6.90[e]
^{8}C	7.71[a]	5.55[a]	5.72[a]	4.38[a]	4.48[a]	4.08[a]	4.08[a], 4.08[a]	f	h
^{9}U	7.72[a]	5.67[a]	5.61[a]	4.30[a]	4.53[a]	4.08[a]	4.08[a], 4.08[a]	g	f
^{10}A	8.24[a]	7.99[a]	5.75[a]	4.70[a]	4.64[a]	4.29[a]	4.08[a], 4.04[a]	f	h
^{11}A	8.14[a]	8.07[a]	5.93[a]	4.67[a]	4.93[a]	4.37[a]	4.28[a], 4.06[a]	f	h
^{12}U	7.65[a]	5.68[a]	7.66[a]	4.30[a]	4.55[a]	4.01[a]	4.09[a], 4.09[a]	g	f
^{13}G	7.84[a]	f	5.74[a]	4.76[a]	4.86[a]	4.35[a]	4.17[a], 4.10[a]	g	h
^{14}A	8.32[a]	8.18[a]	6.05[a]	4.91[a]	4.74[a]	4.64[a]	4.40[a], 4.36[a]	f	h
^{15}G	7.41[a]	f	5.33[a]	b	b	4.36[a]	b	13.13[e]	h
^{16}C	7.70[a]	5.20[c]	5.59[a]	b	b	b	b	f	8.44[e], 6.65[e]
^{17}G	7.53[a]	f	5.79[a]	b	b	4.50[a]	b	12.28[e]	h
^{18}G	7.24[a]	f	5.76[a]	b	b	4.48[a]	b	12.74[e]	h
^{19}G	7.23[a]	f	5.78[a]	b	b	4.48[a]	b	13.29[e]	h
^{20}C	7.59[a]	5.22[c]	5.60[a]	b	b	4.41[a]	b	f	8.58[e], 6.98[e]
^{21}U	7.82[a]	5.57[c]	5.85[a]	4.10[a]	4.22[a]	4.22[a]	b	g	f

[a]Visible in the natural 21mer RNA but could only be assigned unambiguously on the basis of the data from the deuterated analogue.
[b]Not extractable from the NMR spectra of the natural 21mer RNA because of the crowding or lack of sequential connectivity. They are also not extractable from the deuterated counterpart due to the substitution of these protons by deuterium.
[c]Visible only in the natural 21mer RNA because they are substituted with deuterium in the deuterated counterpart.
[e]Have been observed in both natural and deuterated RNAs dissolved in H_2O-D_2O (9:1, v/v) at 21°C.
[f]Unexisting resonance.
[g]Resonance is not observed because of rapid exchange with water.
[h]Unassigned resonance.

All the connectivities seen in the deuterated analogue of 21mer RNA (Figs 2c, 3b and 4b) were typical for a right-handed A-form helix and these connectivity patterns were also found to continue for the nucleotide residues of the loop (Figs 3b and 4b) suggesting that the unpaired loop bases in 21mer RNA form a sort of continuation of the helical stack. Even the NOE connectivities from 1′U12 to 2A11, 1′G15 to 2A14 and 1′A11 to 2A10 are observed (Fig. 3b). In addition, because of unambiguous assignment with the help of deuterated analogue, we also find important peculiar structural feature of the loop as evident by 8A11–1′U9 or 1′G13–8G15 NOE connectivities (Fig. 3b).

We have thus obtained, on average, 18 intra and internucleotidyl NOE constraints per nucleotidyl residue for seven nucleotides in the loop as well as their dihedral constraints for the sugar residues. In addition, we see the typical A-RNA type NOE pattern for the stem part of the 21mer RNA as well as a clear picture of the sugar conformation of the constituent nucleotides in the stem part of the deuterated RNA. This knowledge is now being used for NMR-constrained molecular model building studies, which will be reported elsewhere. Work is in progress to incorporate ^{13}C/^{15}N isotopes specifically in the loop region (i.e. in the 'NMR-window' part) of the 21mer RNA for obtaining additional torsional constraints (33). We are also now extending this work for studying the active sites of ribozymes.

The 'NMR-window' concept described above for a complete sequential assignment of a reasonably large oligo-RNA using the combination of deuterated and natural phosphoramidite building blocks shows that the approach is indeed synthetically and spectroscopically feasible. The deuterated nucleosides are now easily accessible (5) since deuterated sugars can be easily prepared directly in >240 mmol scale in one pot. The two other important problems that are being tackled in our lab are (i) to improve the coupling yield of the phosphoramidites on a large scale solid phase synthesis for large oligo-RNA preparation, and (ii) improvement of the separation techniques that would lead to large oligo-RNA in a pure form in multimilligram quantities.

ACKNOWLEDGEMENTS

We wish to thank the Swedish Board for Technical Development (NUTEK), the Swedish Natural Science Research Council (NFR) and the Swedish Research Council for Engineering Sciences

(TFR) for generous financial support. We would also like to thank Wallenbergsstiftelsen, University of Uppsala and Forskningsrådsnämnden (FRN) for financial support in the purchase of the 500 MHz NMR spectrometer.

REFERENCES

1 Wüthrich, K. (1986) *NMR of Proteins and Nucleic Acids.* Wiley, New York.
2 Aboul-ela, F. and Varani, G. (1995) *Curr. Opin. Biotechnol.*, **6**, 89–95.
3 Dieckmann, T. and Feigon, J. (1994) *Curr. Opin. Struct. Biol.*, **4**, 745–749.
4 Moore, P. B. (1995) *Acc. Chem. Res.*, **28**, 251–256.
5 Földesi, A., Nilson, F. P. R., Glemarec, C., Gioeli, C. and Chattopadhyaya, J. (1992) *Tetrahedron*, **48**, 9033–9072.
6 Földesi, A., Nilson, F. P. R., Glemarec, C., Gioeli, C. and Chattopadhyaya, J. (1993) *J. Biochem. Biophys. Methods*, **26**, 1–26.
7 Yamakage, S.-I., Maltseva, T. V., Nilson, F. P., Földesi, A. and Chattopadhyaya, J. (1993) *Nucleic Acids Res.*, **21**, 5005–5011.
8 Agback, P., Maltseva, T. V., Yamakage, S.-I., Nilson, F. P. R., Földesi, A. and Chattopadhyaya, J. (1994) *Nucleic Acids Res.*, **22**, 1404–1412.
9 Földesi, A., Yamakage, S.-I., Maltseva, T. V., Nilson, F. P., Agback, P. and Chattopadhyaya, J. (1995) *Tetrahedron*, **51**, 10065–10092.
10 Westman, E. and Strömberg, R. (1994) *Nucleic Acids Res.*, **22**, 2430–2431.
11 Markiewicz, W. T. (1979) *J. Chem. Res. (M)*, 181–196.
12 Lyttle, M. H., Wright, P. B., Sinha, N. D., Bain, J. D. and Chamberlin, A. R. (1991) *J. Org. Chem.*, **56**, 4608–4615.
13 Rabi, J. A. and Fox, J. J. (1973) *J. Am. Chem. Soc.*, **95**, 1628–1632.
14 Zhou, X.-X., Welch, C. J. and Chattopadhyaya, J. (1986) *Acta Chem. Scand.*, **B40**, 806–816.
15 Ti, G. S., Gaffney, B. L. and Jones, R. A. (1982) *J. Am. Chem. Soc.*, **104**, 1316–1319.
16 Wu, T. and Ogilvie, K. K. (1987) *Tetrahedron Lett.*, **29**, 4249–4252.
17 Hakimelahi, G. H., Proba, Z. A. and Ogilvie, K. K. (1982) *Can. J. Chem.*, **60**, 1106–1113.
18 Beaucage, S. L. and Caruthers, M. H. (1981) *Tetrahedron Lett.*, **22**, 1859–1862.
19 Sinha, N. D., Biernat, J. and Köster, H. (1983) *Tetrahedron Lett.*, **24**, 5843–5846.
20 Usman, N., Ogilvie, K. K., Jiang, M.-Y. and Cedergren, R. J. (1987) *J. Am. Chem. Soc.*, **109**, 7845–7854.
21 Gasparutto, D., Livache, T., Bazin, H., Duplaa, A.-M., Guy, A., Khorlin, A., Molko, D., Roget, A. and Téoule, R. (1992) *Nucleic Acids Res.*, **20**, 5159–5166.
22 Bodenhausen, G., Kogler, H. and Ernst, R. R. (1984) *J. Magn. Reson.*, **580**, 370–383.
23 Neuhaus, D., Wagner, G., Vasak, M., Kagi, J. H. R. and Wuthrich, K. (1985) *Eur. J. Biochem.*, **151**, 257–273.
24 Maltseva, T. V., Agback, P. and Chattopadhyaya, J. (1993) *Nucleic Acids Res.*, **21**, 4246–4252.
25 Ramesh, V. (1993) *Nucleic Acids Res.*, **21**, 5485–5488.
26 Varani, V. and Tinoco, I. (1991) *Q. Rev. Biophys.*, **24**, 479–532.
27 Heller, S. R. (1968) *Biochem. Biophys. Res. Commun.*, **32**, 998–1001.
28 Wataya, Y. and Hayatsu, H. (1972) *J. Am. Chem. Soc.*, **94**, 8927–8928.
29 Kim, I., Watanabe, S., Muto, Y., Hosono, K., Takai, K., Takaku, H., Kawai,.G., Watanabe, K. and Yokoyama. S. (1995), *Nucleic Acids Res. Symp. Series* , **34**, 123–124. In this work, 90% ^{2}H enrichment was only achieved.
30 Puglisi, J. D., Wyatt, J. R. and Tinoco, I. Jr. (1990) *J. Mol. Biol.*, **214**, 437–453.
31 White, S. A., Nilges, M., Huang, A., Brünger, A. T. and Moore, P. B. (1992) *Biochemistry*, **31**, 1610–1621.
32 Heus, H. A. and Pardi, A. (1991) *J. Am. Chem. Soc.*, **113**, 4360–4361.
33 Allain, F. H.-T. and Varani, G. (1995) *J. Mol. Biol.*, **250**, 333–353.